

Effect of ruthenium doping on superconductivity in Nb_2PdS_5

Q Chen¹, C Y Shen¹, X H Yang¹, X J Yang¹, Y P Li¹, C M Feng^{1,2,3},
Z A Xu^{1,2,3}

¹Department of Physics and State Key Laboratory of Silicon Materials, Zhejiang University, Hangzhou 310027, China

²Zhejiang California International NanoSystems Institute, Zhejiang University, Hangzhou 310058, China

³Collaborative Innovation Centre of Advanced Microstructures, Nanjing 210093, China

E-mail: zhuan@zju.edu.cn

Abstract. We synthesized a series of $\text{Nb}_2\text{Pd}_{1-x}\text{Ru}_x\text{S}_5$ polycrystalline samples by solid-state reaction method and investigated systematically the Ru doping effect on superconductivity by transport and magnetic measurements. It is found that superconductivity is enhanced with Ru doping and the superconducting transition temperature (T_c) reaches a maximum of 6.86 K at $x = 0.2$. Ru doping is regarded as the hole-type doping similar to the case of Ir doping. The evolution of T_c^{mid} with Ru doping is compared with the case of Ir or Ag doping.

1. Introduction

The recent discovery of superconductivity in the new transition metal-chalcogenide compound Nb_2PdS_5 with $T_c \sim 6$ K has attracted much attention[1]. This quasi-one-dimensional(Q1D) material which is argued to be a multi-band superconductor[1, 2, 3, 4] has remarkably high and anisotropic upper critical field ($H_{c2}^{\parallel b} > 37$ T). Chemical substitution has been investigated in this T_2PdCh_5 (T = Nb or Ta, Ch = S or Se) system and superconductivity was found at 2.5 K and 6 K in Ta_2PdSe_5 [3] and Ta_2PdS_5 [5], respectively. Partial substitution of Pd by Ni[6] or Ir[7] has slightly enhanced T_c but superconductivity is suppressed in the cases of Pt-for-Pd doping [6] or Ag-for-Pd doping[7], and Se-for-S doping [8]. However, the feature of large H_{c2} relative to T_c which surpasses by far the expected Pauli limiting field ($H_{c2} = 1.84 T_c$ [9]) is found to be robust against these substitutions. This common feature provide a strong evidence of unconventional superconductivity in this system.

The band structure calculations[1, 4, 10] present that the Fermi surface of Nb_2PdS_5 is composed of multiple sheets and this system is in proximity to a magnetically or charge density wave(CDW) ordered state due to the nesting properties of those Q1D fermi surface sheets. The change in d electron population in the Pd site is expected to flatten the Q1D fermi surface sheets and thus it may enhance the nesting properties and the proposals for unconventional superconducting pairing scenario were suggested[1, 4]. Moreover, it is also suggested that the strong spin-orbit coupling associated with the heavy Pd element could lead to the high H_{c2} [5, 11]. Through controlling SOC by Pt and Ni partial substitutions on the Pd sites, H_{c2}/T_c is found to be tunable, indicating a crucial role of SOC on the enhancement of H_{c2} [6, 12]. These theoretical



and experimental studies have verified the importance of the presence of Pd ions with a large Z number to the unconventional properties. Recently, it has been reported that the charge carrier density (or band filling) which can be modulated by hole(electron)-type doping could be a crucial factor to tune superconductivity[7] in this system. So far, the origin of large H_{c2} and exotic superconductivity in $T_2\text{PdCh}_5$ is far from conclusive.

In this paper, we investigate the doping effect on the Pd site by heterovalent transition metal ruthenium. The Ru doping is considered as a hole-type dopant but with weaker SOC compared to the Ir doping, thus it may help on distinguishing the different roles of charge carrier density and SOC upon superconductivity. The evolution of superconductivity is obtained by measuring electrical resistivity and magnetic susceptibility for $\text{Nb}_2\text{Pd}_{1-x}\text{Ru}_x\text{S}_5$. T_c reaches a maximum of 6.86 K at $x = 0.2$. The superconducting window is wide, indicating a robust superconductivity in Nb_2PdS_5 .

2. Experimental details

We synthesized a series of $\text{Nb}_2\text{Pd}_{1-x}\text{Ru}_x\text{S}_5$ polycrystalline samples by usual solid-state reaction method using stoichiometric amounts of powders of Nb (99.99%), Pd (99.99%), Ir, Ru or Ag (99.99%), and S (99.9%). All the starting materials were thoroughly ground and pressed into pellets and then sealed in evacuated quartz tubes. The quartz ampoules were slowly heated to 1073~1123 K and held for 48 h. This procedure was finally repeated again for homogeneity.

Powder x-ray diffraction (XRD) was carried out at room temperature on a PANalytical X-ray diffractometer using $\text{Cu K}\alpha$ radiation, and lattice constants were determined using the program X'Pert HighScore. Electrical resistivity was measured by a standard four-terminal method using Oxford-15 T cryostat with Keithley 2400 source-measure meters and 2182A nanovoltmeters.

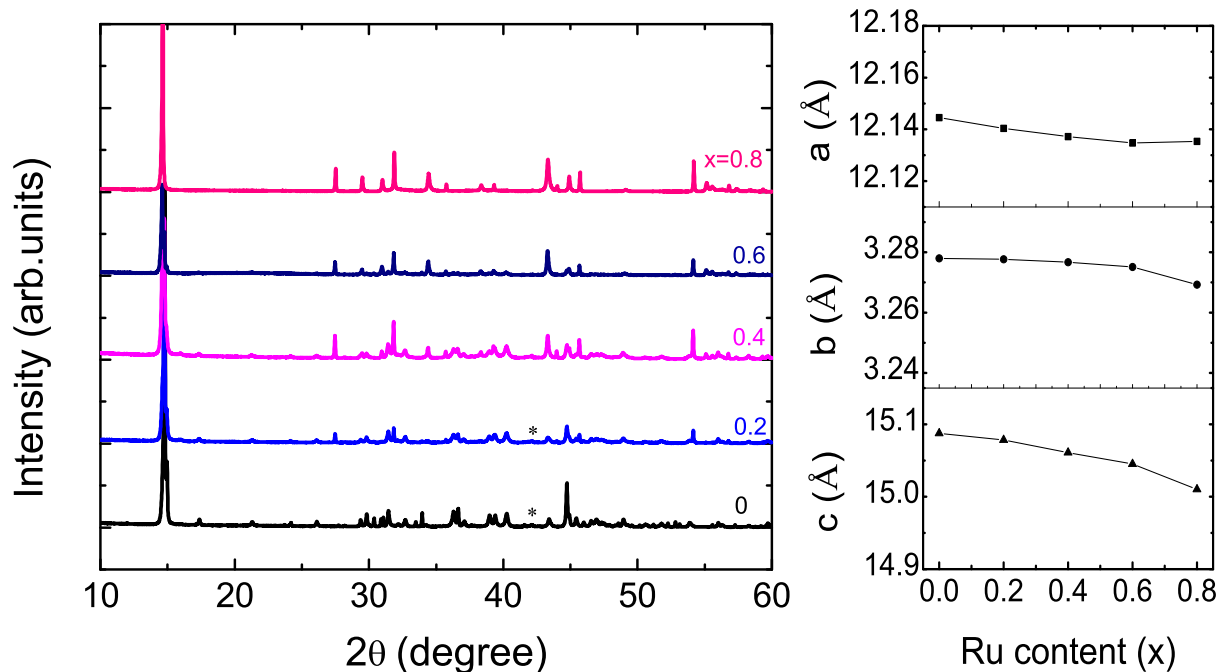


Figure 1. Left panel: room temperature powder X-ray diffraction patterns for $\text{Nb}_2\text{Pd}_{1-x}\text{Ru}_x\text{S}_5$ with $x = 0, 0.2, 0.4, 0.6$ and 1 , respectively. Right panel: lattice constants as a function of nominal doping content x .

3. Result and discussion

Fig. 1 shows the XRD patterns of $\text{Nb}_2\text{Pd}_{1-x}\text{Ru}_x\text{S}_5$ ($x = 0, 0.2, 0.4, 0.6, 1$). All the main peaks can be well indexed with a monoclinic structure (space group C2/m), except for a few minor peaks due to unknown impurities marked by the asterisks. The variation of lattice parameters was shown in the right panel. It is found that a and b remain almost constant while the c -axis shrinks significantly with increasing Ru content. This observation indicates that Ru atoms are successfully doped into this compound which is consistent with the smaller ion radius of Ru compared to Pd.

The temperature-dependent resistivity is shown in Fig. 2. The resistivity at $T = 300$ K ranges from $1.55 \text{ m}\Omega\cdot\text{cm}$ to $4.6 \text{ m}\Omega\cdot\text{cm}$. For the undoped compound ($x = 0$), the resistivity decreases slowly with decreasing temperature and then shows a sharp drop around $T_c \sim 6$ K. This metallic behavior is consistent with previous reports[1][7]. Upon doping with Ru, a small upturn shows up at low temperature which can be ascribed to Anderson localization[5] or grain boundary effect[13]. The inset of Fig. 2 is the enlarged plot of resistivity versus T , showing the variation of superconducting transition. Superconductivity was firstly enhanced then suppressed with further doping which resembles the case of Ir doping [7].

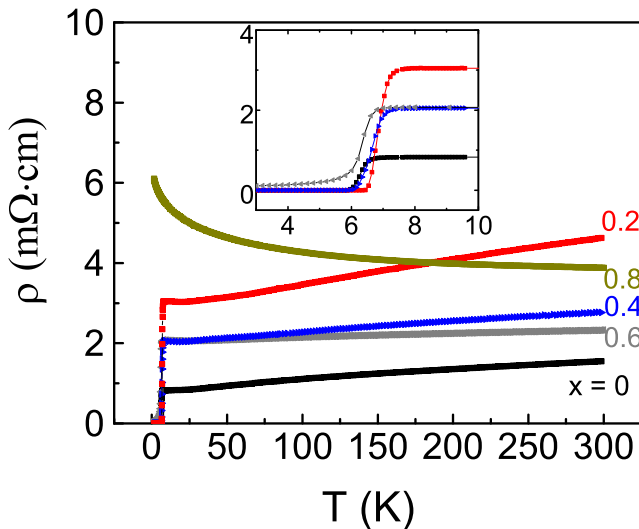


Figure 2. Temperature dependence of the electrical resistivity of $\text{Nb}_2\text{Pd}_{1-x}\text{Ru}_x\text{S}_5$. Inset: the enlarged plot of resistivity around the superconducting transition temperatures.

Figure. 3 presents temperature dependence of magnetic susceptibility. The samples with $0 \leq x \leq 0.4$ show strong diamagnetic signal confirming bulk superconductivity. The transition temperature is consistent with the resistivity measurements (shown in fig. 4). For $x = 0.8$, superconductivity no longer survives.

According to our previous work[7], partial substitution of Pd by Ir which can be considered as hole-type doping could obviously increase T_c for low Ir content, while Ag doping which is regarded as electron-type doping destroys superconductivity quickly. It is interesting to compare the effect of Ru doping with Ir doping both of which are regarded as hole-type dopants. Since the strength of SOC is proportional to Z^4 , where Z is the atomic mass number, Ru doping may hardly change SOC associated with Pd site, while Ir or Pt doping could increase SOC in the system [6, 12]. Therefore we may distinguish the effect of SOC from charge carrier density through comparing Ru doping and Ir doping.

Based on the resistivity and magnetic measurements, a phase diagram of T_c vs. doping level is shown in Fig. 4, the data of Ir or Ag doping are plotted for comparison. Circle symbols stand for the characteristic temperature T_c^{mid} where $\rho(T)$ drops to 50% of the normal state value. Ru and Ir doping are shown by hollow symbols while Ag doping is in solid character. Pentagonal symbols represent superconducting transition temperature derived from magnetic

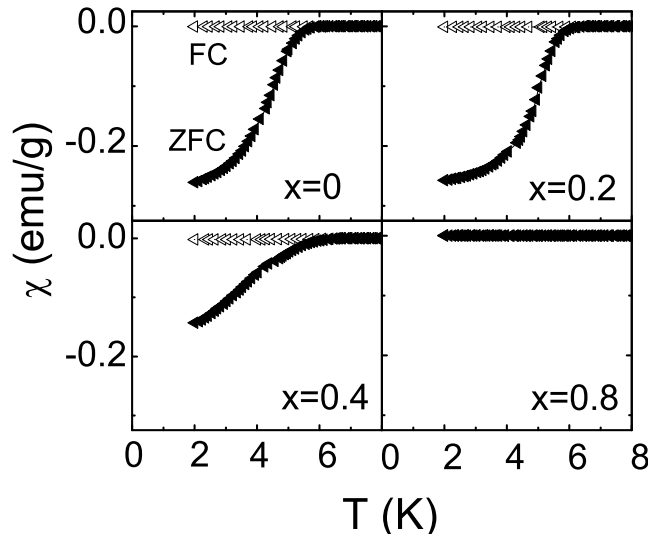


Figure 3. Temperature dependence of magnetic susceptibility measured under $H = 10$ Oe for $\text{Nb}_2\text{Pd}_{1-x}\text{R}_x\text{S}_5$ ($x = 0, 0.2, 0.4,$ and 0.8).

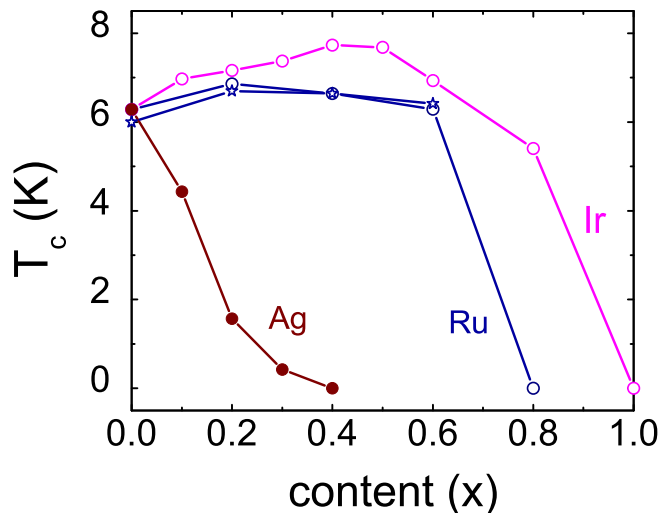


Figure 4. The phase diagram of transition temperature T_c as a function of doping level x . The blue, magenta and wine circle lines stand for T_c^{mid} of Ru, Ir and Ag doped $\text{Nb}_2\text{Pd}_{1-x}\text{R}_x\text{S}_5$, respectively. Pentagonal symbols represent T_c extracted from magnetic susceptibility data.

susceptibility. It can be found that superconductivity is enhanced with a maximum T_c^{mid} of 6.86 K by Ru ($x = 0.2$) doping, and 7.73 K by Ir ($x = 0.4$) doping, respectively. Both Ru and Ir doping are expected to increase the hole-type carrier density, which may drive the system far away from the magnetic order or a possible CDW order and thus favor superconductivity, while the electron-type dopings (i.e., Ag doping) have an opposite effect. In this scenario, we could understand why T_c initially increases for both Ru doping and Ir doping. However, the maximum of T_c is even higher and the superconducting range (up to x of 0.8) is wider for the Ir doping case. We proposed that the enhanced SOC strength due to heavier Ir may account for this difference. This result implies that not only the charge carrier density but also SOC could also play an important role in controlling superconductivity of Nb_2PdS_5 . It should also be noted that superconductivity can survive up to very high doping level in the cases of Ru or Ir doping, which demonstrates that T_c is quite robust upon disorder in the hole-type doping, as compared with the iron-based superconductors $\text{LaFe}_{1-x}\text{Co}_x\text{AsO}$ [14] and $\text{BaFe}_{2-x}\text{Ni}_x\text{As}_2$ [15]. Careful studies on the single-crystalline $\text{Nb}_2\text{Pd}_x\text{S}_{5-\delta}$ have found that superconductivity occurs in a wide range of Pd ($0.6 < x < 1$) and S ($0 < \delta < 0.61$) contents[16], suggesting again that superconductivity in this system is very robust.

4. Conclusion

In summary, we studied the Ru doping effect on superconductivity in Nb_2PdS_5 and superconductivity with a maximum T_c^{mid} of 6.86 K at $x = 0.2$ has been observed. Bulk superconductivity is confirmed by magnetic measurements. An electronic phase diagrams is presented showing the enhancement of T_c by partial substitution of Pd by Ru and the comparison with the Ir or Ag doping is made, which indicates that the charge carrier density as well as SOC has a significant effect on the superconductivity.

Acknowledgments

This work is supported by the National Basic Research Program of China (Grant Nos. 2014CB921203 and 2012CB927404), NSF of China (Contract Nos. U1332209 and 11190023), the Ministry of Education of China (Contract No. 2015KF07), and the Fundamental Research Funds for the Central Universities of China.

References

- [1] Zhang Q et al (2013) "Superconductivity with extremely large upper critical fields in $\text{Nb}_2\text{Pd}_{0.81}\text{S}_5$." *Sci. Rep.* **3**.
- [2] Zhang Q R, Rhodes D, Zeng B, Besara T, Siegrist T, Johannes M D, and Balicas L (2013) "Anomalous metallic state and anisotropic multiband superconductivity in $\text{Nb}_3\text{Pd}_{0.7}\text{Se}_7$." *Phys. Rev. B* **88**(2), 024508.
- [3] Zhang J, Dong J K, Xu Y, Pan J, He L P, Zhang L J and Li S Y (2015) "Superconductivity at 2.5 K in the new transition-metal chalcogenide $\text{Ta}_2\text{Pd}_x\text{Se}_5$." *Supercond. Sci. Tech.* **28**(11), 115015.
- [4] Singh D J (2013) "Electronic structure and upper critical field of superconducting $\text{Ta}_2\text{Pd}_x\text{S}_5$." *Phys. Rev. B* **88**(17), 174508.
- [5] Lu Y, Takayama T, Bangura A F, Katsura Y, Hashizume D and Takagi H (2013) "Superconductivity at 6 K and the violation of Pauli limit in $\text{Ta}_2\text{Pd}_x\text{S}_5$." *J. Phys. Soc. Jpn* **83**(2), 023702.
- [6] Zhou N et al (2014) "Controllable spin-orbit coupling and its influence on the upper critical field in the chemically doped quasi-one-dimensional Nb_2PdS_5 superconductor." *Phys. Rev. B* **90**(9), 094520.
- [7] Shen C Y, Si B Q, Bai H, Yang X J, Tao Q, Cao G H and Xu Z A (2016) "Pd site doping effect on superconductivity in $\text{Nb}_2\text{Pd}_{0.81}\text{S}_5$." *Europhys. Lett.* **113**(3), 37006.
- [8] Niu C Q et al (2013) "Effect of selenium doping on the superconductivity of $\text{Nb}_2\text{Pd}(\text{S}_{1-x}\text{Se}_x)_5$." *Phys. Rev. B* **88**(10), 104507.
- [9] Clogston A M (1962) "Upper limit for the critical field in hard superconductors." *Phys. Rev. Lett.* **9**(6), 266.
- [10] Seunghyun K et al (2013) "Enhanced upper critical fields in a new quasi-one-dimensional superconductor $\text{Nb}_2\text{Pd}_x\text{Se}_5$." *New. J. Phys.* **15**(12), 123031.
- [11] Carbotte J P (1990) "Properties of boson-exchange superconductors." *Rev. Mod. Phys.* **62**(4), 1027.
- [12] Werthamer N R, Helfand E and Hohenberg P C (1966) "Temperature and purity dependence of the superconducting critical field, H_{c2} . III. Electron spin and spin-orbit effects." *Phys. Rev.*, **147**(1), 295.
- [13] Carrington A and Cooper J R (1994) "Influence of grain-boundary scattering on the transport properties of a high- T_c oxide superconductor." *Physica C: Superconductivity.* **219**(1), 119-22.
- [14] Wang C et al (2009) "Effects of cobalt doping and phase diagrams of $\text{LFe}_{1-x}\text{Co}_x\text{AsO}$ (L = La and Sm)." *Phys. Rev. B* **79**(5), 054521.
- [15] Li L J et al (2009) "Superconductivity induced by Ni doping in BaFe_2As_2 single crystals." *New. J. Phys.* **11**(2), 025008.
- [16] Yu H, Zuo M, Zhang L, Tan S, Zhang C, and Zhang Y (2013). "Superconducting fiber with transition temperature up to 7.43 K in $\text{Nb}_2\text{Pd}_{1-x}\text{S}_5$ ($0.6 < x < 1$)." *J. Am. Chem. Soc.* **135**(35), 12987-89.